

Molecular dissection of the multifunctional poliovirus RNA-binding protein 3AB

WENKAI XIANG, ANDREA CUCONATI, ANIKO V. PAUL, XUEMEI CAO, and ECKARD WIMMER

Department of Molecular Genetics and Microbiology, School of Medicine,
State University of New York at Stony Brook, Stony Brook, New York 11794-5222, USA

ABSTRACT

Genome replication of poliovirus, as yet unsolved, involves numerous viral polypeptides that arise from proteolysis of the viral polyprotein. One of these proteins is 3AB, an RNA-binding protein with multiple functions, that serves also as the precursor for the genome-linked protein VPg (=3B). Eight clustered charged amino acid-to-alanine mutants in the 3AB coding region of poliovirus were constructed and analyzed, together with three additional single-amino acid exchange mutants in VPg, for viral phenotypes. All mutants expressed severe inhibition in RNA synthesis, but none were temperature sensitive (*ts*). The 3AB polypeptides of mutants with a lethal phenotype were overexpressed in *Escherichia coli*, purified to near homogeneity, and studied with respect to four functions: (1) ribonucleoprotein complex formation with 3CD^{pro} and the 5'-terminal cloverleaf of the poliovirus genome; (2) binding to the genomic and negative-sense RNA; (3) stimulation of 3CD^{pro} cleavage; and (4) stimulation of RNA polymerase activity of 3D^{pol}. The results have allowed mapping of domains important for RNA binding and the formation of certain protein-protein complexes, and correlation of these processes with essential steps in viral genome replication.

Keywords: 3AB; poliovirus RNA replication; protein-protein interaction; protein-RNA interaction; systematic mutagenesis

INTRODUCTION

Although genome replication of poliovirus, the prototype of Picornaviridae, has been studied for decades, two crucial steps in this process, initiation of plus and minus strand synthesis, remain unsolved. The poliovirus genome, a single-stranded, positive-sense RNA, approximately 7,440-nt long, has a heteropolymeric, VPg-linked 5' end and a homopolymeric, polyadenylylated 3' end (Wimmer et al., 1993). Covalent attachment of VPg to all newly formed viral RNA is essential for genome replication (Nomoto et al., 1977; Kuhn et al., 1988b; Reuer et al., 1990). The difference of the termini of the viral RNA both in sequence and structure make it likely that initiation of synthesis of minus and plus RNA occurs by different processes. Indeed, distinct higher-order structures have been identified near the termini of the RNA: a characteristic cloverleaf at the 5' end (Fig. 1A) (Rivera et al., 1988; Andino et al., 1990a)

and a pseudoknot at the 3' end (Pilipenko et al., 1992; Jacobson et al., 1993). The integrity of both the cloverleaf (Racaniello & Meriam, 1986; Kuge & Nomoto, 1987; Andino et al., 1990a, 1990b; Rohll et al., 1994) and the pseudoknot (Pilipenko et al., 1992; Jacobson et al., 1993) is essential for RNA replication (Wimmer et al., 1993), an observation implying that the structures serve as replication signals.

The 5' nontranslated region (NTR) of poliovirus RNA is unusually long (10% of the viral genome) and harbors, in addition to the cloverleaf, a second structural element, the internal ribosomal entry site (IRES) (Fig. 1A) (Wimmer et al., 1993). The IRES is cardinal for the viral cap-independent initiation of viral protein synthesis (Jang et al., 1988; Pelletier & Sonenberg, 1988). The poliovirus IRES has also been reported to play a role in genome replication (Borman et al., 1994), although it can be replaced with the IRES of encephalomyocarditis virus (EMCV) (Alexander et al., 1994; Xiang et al., 1995), a genetic element very different in sequence and structure, but similar in function (Wimmer et al., 1993).

Translation of the poliovirus genome yields a polyprotein that is processed by virus-encoded proteinases

Reprint requests to: Eckard Wimmer, Department of Molecular Genetics and Microbiology, School of Medicine, State University of New York at Stony Brook, Stony Brook, New York 11794-5222, USA; e-mail: wimmer@asterix.bio.sunysb.edu.

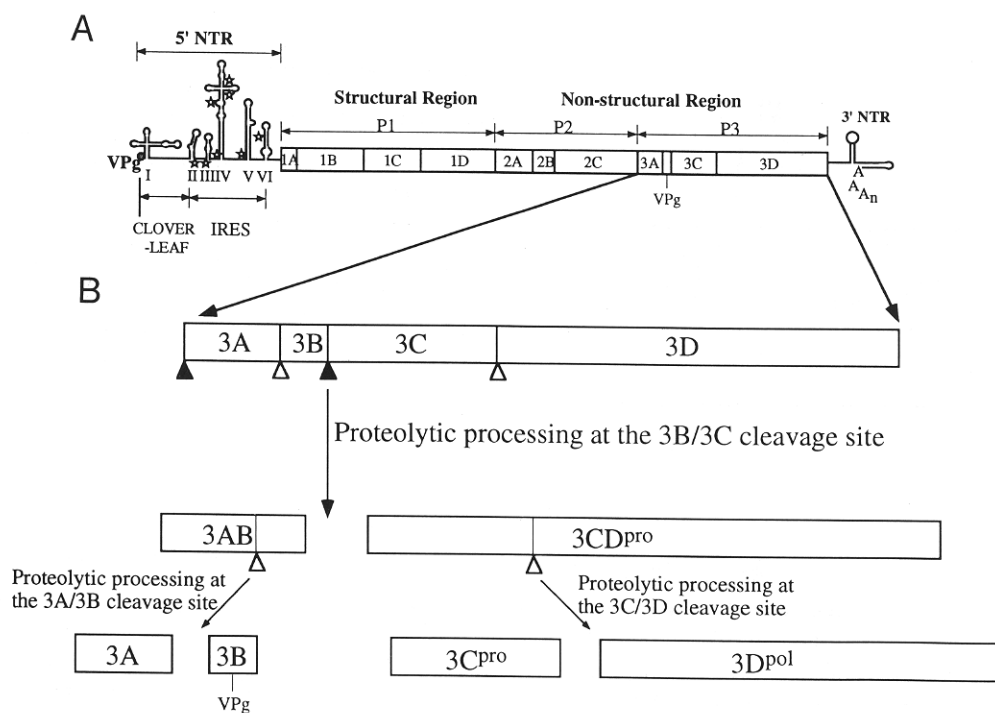


FIGURE 1. Structure of polioviral genomic RNA. **A:** RNA structural domains in the 5' NTR are indicated by Roman numerals. Stars indicate the position of noninitiating AUG triplets. **B:** Enlargement of the P3 nonstructural precursor and its processing products. Closed and open triangles indicate rapidly and slowly processed Q/G cleavage sites, respectively.

into structural and nonstructural proteins (Harris et al., 1990; Lawson & Semler, 1992). Interestingly, some cleavage intermediates attain relatively long half-lives and perform functions distinct from those of their cleavage products (Wimmer et al., 1993 and references therein). The primary cleavage products of the P3 region may serve as striking examples (Fig. 1B). 3AB and 3CD^{pro} are generated rapidly, but only slowly cleaved to 3A+VPg and 3C^{pro}+3D^{pol}, respectively. 3AB, a non-specific RNA-binding protein (Paul et al., 1994a), and 3CD^{pro}, a proteinase, form a complex in solution (Molla et al., 1994). This complex can enter different pathways of biochemical events: (1) acceleration of *cis* cleavage of 3CD^{pro} to 3C^{pro} and 3D^{pol}, the RNA polymerase (Molla et al., 1994); (2) cleavage of membrane-bound 3AB into 3A and VPg (Lama et al., 1994); and (3) formation of a ribonucleoprotein (RNP) complex with the 5' cloverleaf structure with high affinity and specificity (Harris et al., 1994). Recent data have shown that the [3AB/3CD^{pro}/cloverleaf]-RNP is an essential component in viral RNA replication (Xiang et al., 1995). Finally, 3AB and 3D^{pol} can form a complex (Molla et al., 1994; Paul et al., 1994a) that results in the multifold stimulation of 3D^{pol} RNA polymerase activity ([3AB/3D]^{superpol}; Lama et al., 1994; Paul et al., 1994a).

The involvement of 3AB in RNA replication has been suggested previously on the basis of genetic analyses (Bernstein et al., 1986; Bernstein & Baltimore, 1988; Giachetti & Semler, 1991; Giachetti et al., 1992). More-

over, a change of the Tyr-Thr to Phe-Ala residues in VPg has led to a lethal phenotype of the constructs, an observation implying that the covalent linkage between VPg and RNA is required for replication (Kuhn et al., 1988a; Reuer et al., 1990; Cao & Wimmer, 1995a). Finally, poliovirus RNA with two tandemly arranged VPgs is only quasi-infectious, and its replication leads to the complete deletion of the 3C^{pro}-proximal VPg (Cao et al., 1993; Cao & Wimmer, 1995b). The insertion of a second VPg has been found to cause aberrant polyprotein processing, which suggests that the arrangement of structural domain in P3 region of the polyprotein is sensitive to perturbation (Cao et al., 1993; Cao & Wimmer, 1995b).

Previous analyses have revealed that 3AB is strongly basic and water insoluble, two properties resulting from numerous basic residues and a highly hydrophobic domain of 22 residues, respectively (see Fig. 2A; Semler et al., 1982; Lama et al., 1994). It has been suggested that the hydrophobic domain is responsible for the membrane association of 3AB in infected cells (Semler et al., 1982; Datta & Dasgupta, 1994). This fits the observation that poliovirus genome replication occurs in membranous complexes to which the basic VPg would have to be delivered for initiation of RNA synthesis (Takegami et al., 1983; Takeda et al., 1986; Bienz et al., 1990).

Altogether, 3AB must be considered a multifunctional protein that plays a central role in poliovirus rep-

evidence that the interactions between 3AB, 3CD^{pro}, 3D^{pol}, and viral RNA structures are essential for genome replication.

RESULTS

Site-directed mutagenesis of poliovirus 3AB coding region

Hydropathy analysis of poliovirus-encoded 3AB demonstrates that polar amino acid residues are distributed around both termini of the protein, whereas an internal 22-amino acid stretch near the C-terminus of 3A is quite hydrophobic (Fig. 2A). The contrast in hydrophilicity suggests that the charged sequences may map to regions involved in protein-protein and/or protein-polynucleotide interaction, whereas the hydrophobic stretch may enable 3AB to associate with membranes. In order to investigate the functionality of the charged regions, charged residues in those regions were changed to alanines (Fig. 2A). The number of nucleotide and amino acid changes for each clustered charge-to-alanine mutation are given in Figure 2B. Mutations were introduced by deoxyoligonucleotide-directed mutagenesis (Kunkel et al., 1987) into the segments of the 3AB region present in phagemid vectors (see the Material and methods). Each of the mutations was transferred back to the full-length poliovirus cDNA clone. In addition, we included into our analyses amino acid substitutions of an arginine residue near the C-terminus of 3B that had been constructed previously by Kuhn et al. (1988b) (R17K, R17Q, R17E; Fig. 2B).

Run-off transcripts using linearized cDNA clones were prepared as described previously (Xiang et al., 1995) and tested as translational templates in HeLa cell-free extracts (Molla et al., 1991). Compared to the translation of the wt transcript, similar translation efficiencies and processing patterns were observed in PAGE analysis for all mutant RNAs (data not shown), an observation confirming intact open reading frames (ORF) of the mutant polyproteins. However, several of the mutated 3AB polypeptides displayed slightly altered mobility in the polyacrylamide gel (data not shown; see also below).

Phenotypic characterization of the mutant genomes

Equal amounts of in vitro-produced RNA transcripts derived from the full-length clones were transfected into HeLa R19 cell monolayers at 37 °C. After 20 h, cytopathic effects (CPE) were visible in monolayers transfected with PV1(M) transcripts. CPE could also be detected in cells after 36, 45, and 48 h posttransfection with 3AB-M7, -M8, and -M9 transcripts, respectively. The cells transfected with the remaining transcripts

showed no CPE, even after four days of incubation (Fig. 2B).

To determine whether infectious viruses were generated from the RNA transfections, the cell lysates harvested at the time when CPE was most pronounced (20–72 h posttransfection) were subjected to plaque assays on R19 HeLa cell monolayers. W1-PV1(M) yielded large-size plaques, as expected, whereas W1-PV1-3AB-M7, W1-PV1-3AB-M8, and W1-PV1-3AB-M9 yielded small-size plaques. In contrast, no infectious virus was detected from cells transfected with the remaining transcripts. This negative result was reproducible. All the transcripts were transfected into cell cultures and incubated also at 32.5 or 39.5 °C to check for possible *ts* phenotypes. Cell lysates were subsequently analyzed by plaque assays at both temperatures. The results were similar to those obtained at 37 °C. Infectious virus was obtained with constructs PV1-3AB-M7, 8, and 9, and the corresponding viruses (W1-PV1-3AB-M7, 8, and 9) proliferated at all three temperatures tested with no apparent *ts* phenotype. None of the constructs that were lethal at 37 °C yielded virus at the other temperatures.

The plaque phenotypes of the viable mutant viruses were generally uniform and stable through four passages of infection. The viral RNAs extracted from either the first or the fourth passage were subjected to RNA sequencing of the 3AB encoding region, and there were no changes in the genotypes found. However, whether the phenotypes of these viruses are solely the result of the 3AB mutations, or whether the 3AB M7, M8, and M9 viruses harbor additional second-site mutations remains the subject of future studies.

In order to measure plus-strand RNA synthesis in transfected cells, an [α -³²P]UTP-labeled polyribonucleotide probe was prepared that is complementary to the 5' end of the poliovirus genomic RNA (see the Materials and methods). An RNA dot-blot assay was performed using RNA samples extracted from transfected HeLa cells at either 3.5 or 25 h posttransfection. PV1(M) transcripts yielded about 100 ng of the positive-sense RNA at 25 h, whereas the three viable mutant transcripts generated signals at a range of 10–50 ng (Fig. 3A). Notably, the mutant M19 transcripts that did not yield virus also showed weak but clearly detectable plus sense RNA signals. No such signal, however, could be detected in the cells transfected with the remaining mutant transcripts.

During poliovirus infection, the ratio of viral plus-over minus-strand RNAs is, on the average, 50 to 1 (Novak & Kirkegaard, 1991; Wimmer et al., 1993). Therefore, the method of reverse transcription-coupled PCR (RT/PCR), which is more sensitive than dot-blot analysis, was used to detect minus-strand RNAs. To determine if residual plasmid DNA could give rise to the PCR-amplified products, RNA samples isolated 3.5 h posttransfection were directly subjected to PCR reaction (leaving out the step of reverse transcription).

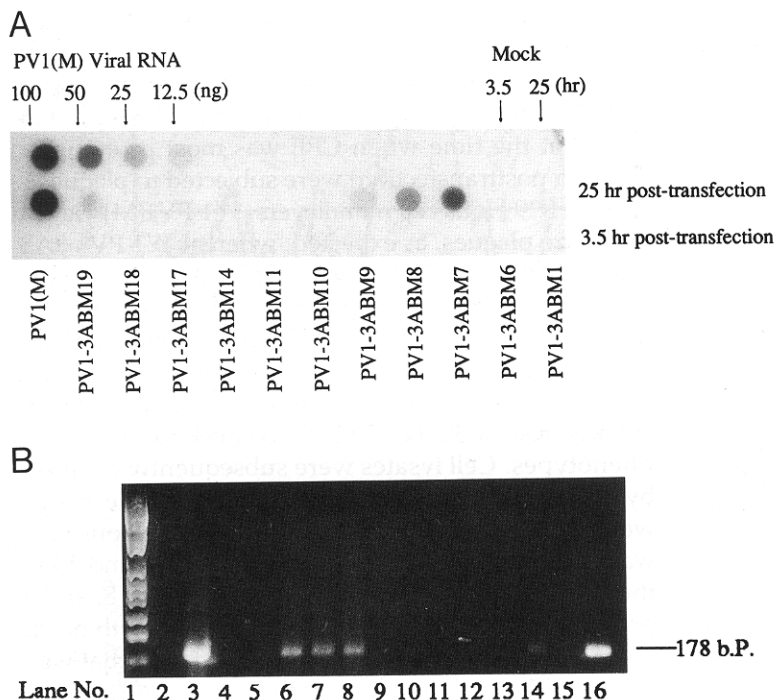


FIGURE 3. Detection of RNA synthesis in cells transfected with wild-type or mutant transcripts. **A:** Measurement of plus-strand RNA synthesis by dot-blot assay. The four wells at the top left side contained differing amounts of PV1(M) virion RNA as controls, whereas the two at right are samples from the mock infected cells. **B:** RT/PCR analysis of negative-strand RNA synthesis from the cells 25 h posttransfection; 12.5 μ L of 50 μ L total PCR products from each sample was loaded. Lane 1, DNA molecular marker VI from Boehringer Mannheim Co.; lane 2, PCR product (without previous reverse transcription step) from PV1(M) RNA transfected cells at 3.5 h posttransfection; lanes 3–15, detection of negative-strand RNA from PV1(M), PV1-3AB-M1, M6, M7, M8, M9, M10, M11, M14, M17, M18, and M19, and mock transfected cells, respectively; lane 16, PCR product using plasmid pT7PV1(M) as template.

No PCR product was apparent in an analysis of RNA isolated from transfections with wt PV (Fig. 3B, lane 2) or mutant transcripts (data not shown) when the RT step was omitted. At 25 h posttransfection, minus strands from cells transfected with PV1(M)-specific transcripts could be easily detected (Fig. 3B, lane 3). This was true also for the three viable (lanes 6–8) and for the lethal M19 (lane 14) transcript RNAs, although the signals were weaker. In contrast, no signal was obtained from the total RNA, which was extracted from cells transfected with the other lethal mutant RNAs (lanes 4–5 and lanes 9–13).

Purification of mutant 3AB proteins

RNAs of all mutant constructs showed normal processing patterns when translated in vitro (data not shown). Therefore, the phenotypes described above are likely to be the result of impaired functions of 3AB in RNA replication. However, we cannot rigorously exclude the possibility that the effect of some 3AB mutations is related to a step in protein processing that functions only in vivo. In order to characterize the nature of functional loss of 3AB, coding regions of eight lethal constructs (M6, 10, 11, 1, 14, 17, 18, 19; Fig. 2B) were cloned into a protein expression vector pET11b, and the integrity of the full-length 3AB encoding sequence was verified by sequencing analysis. The polypeptides were expressed in *Escherichia coli* and purified (see the Materials and methods, and reference therein).

Similar to the properties of wt 3AB, all variant 3AB polypeptides were membrane-associated in *E. coli* ly-

sates. Therefore, they were solubilized in Nonidet P-40, followed by chromatography through a DEAE-cellulose column at pH 8.5, where they appeared in the flow-through fractions. However, distinct differences to wt 3AB became apparent upon chromatography on the cation exchange resin S-sepharose. 3AB-M14 and 3AB-M18 failed to bind to the resin (Fig. 5A), an observation suggesting that the substitution of lysine-lysine (K9, K10) with alanine-alanine (3AB-M14) or of arginine (R17) with glutamic acid (3AB-M18) in the VPg-domain had abolished the interaction between the positively charged protein and the negatively charged resin. Other mutant proteins bound to the column with intermediate affinities: none of them eluted with buffer containing 10 mM NaCl; 3AB-M6, M11, M17, and M1 eluted with the 100 mM NaCl buffer, whereas 3AB-M10 and M19 were eluted similar to wt 3AB (Fig. 4A; see the Materials and methods).

The peak fractions containing these mutant proteins were pooled. Analysis by SDS-PAGE revealed >95% purity, and some of the proteins showed altered mobility (Fig. 4B), which is consistent with the results obtained by in vitro translation of transcript RNA (data not shown).

RNA-binding activity and [3AB/3CD^{pro}/cloverleaf]-RNP formation with 3AB mutant proteins

3AB has been found to be a nonspecific RNA-binding protein by three different experimental methods. Gel-shift, UV-crosslinking, and filter-binding assays all showed it binding to the 3'-terminal sequences of po-

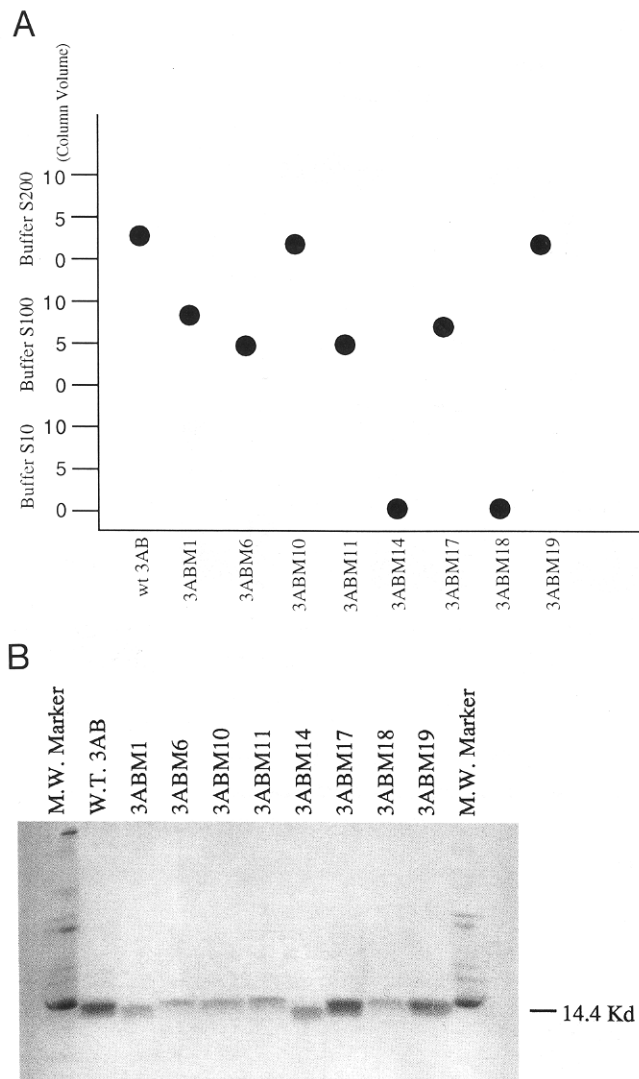


FIGURE 4. Purification of wt and mutant 3ABs. **A:** Position of peak fraction eluted from the S-sepharose column. After application of different 3AB samples from DEAE-cellulose column, the S-sepharose column was washed with 10 column volumes of buffer S10, S100, and S200, sequentially (see the Materials and methods). The positions of the peak fractions were detected through SDS-PAGE analysis. Solid circles indicate the position of peak fractions for each mutant (e.g., the peak wt 3AB eluent is around 2 column volumes wash of buffer S200). **B:** Purity and mobility of wt and mutant 3ABs on 15% SDS-polyacrylamide gel. The gel was stained with Coomassie Brilliant Blue R-250.

liovirus RNA (Harris et al., 1994; Paul et al., 1994a). Gel-shift and UV-crosslinking assays showed that heteropolymeric segments from other parts of genomic or negative-sense RNA can also be the binding target of 3AB (unpubl. result). We have carried out 3AB binding experiments using ^{32}P -labeled cloverleaf RNA prepared as probe (Fig. 5). Gel-shift assays were carried out with increasing amounts (0.4, 0.8, and 1.6 μg) of purified wt 3AB, mutant 3ABs M1, M6, M10, M11, M14, M17, M18, and M19 (Fig. 5A). Whereas wt and mutants M1, 6, 10, 11, and 19 bound to the probe at all

concentrations, that of M14 (Fig. 5A, lanes 17–19) and M18 (Fig. 5A, lanes 23–25) did not bind the RNA at all. Only at the highest concentration tested could M17 maximally shift all the probe. Meanwhile, 3AB M1 could retard the probe at the lowest concentration only to approximately 50% (lane 5), and it thus displayed a weaker binding affinity than wt 3AB. However, filter-binding assays remain to be done to determine more accurately the relative binding affinities. Nevertheless, a cursory inspection of the data in Figure 5A leads us to suggest a binding order as follows: (M14, M18) < M17 < M1 < (M10, M11) < (M6, M19, wt). Binding of wt 3AB to the probe was abolished by adding either yeast tRNA (lane 29) or 2C RNA (lane 30; 2C RNA is a 100-nt plus sense transcript derived from the coding region for protein 2C) as a competitor. This allowed us to conclude that the binding of 3AB to the RNA probe was nonspecific.

In the presence of 1,000-fold excess of tRNA, purified poliovirus-encoded 3CD^{PRO} alone (Fig. 5B, lane 3), like purified 3AB alone (Fig. 5B, lane 2), has no RNA-binding properties (see lane 1; RNA probe alone). However, 3AB plus 3CD^{PRO} form an RNP with the 5'-terminal cloverleaf, as shown previously (lane 4; Harris et al., 1994; Xiang et al., 1995). A 100-fold excess of 2C competitor RNA did not affect RNP formation (lane 31). In sharp contrast, M14 converted only a small fraction of the probe to an RNP complex at the top of the gel (lane 19), whereas M18 failed to form an RNP complex altogether (lane 25). In the continued presence of 1,000-fold excess of tRNA, we then analyzed the effect of excess, nonlabeled cloverleaf on RNP formation with 3CD^{PRO} and different 3AB preparations. Twenty-fold molar excess of cloverleaf RNA had some weak effect on complex formation with M19 (lane 29) and M6 (lane 11), an increasing inhibitory effect with M11 (lane 17), M10 (lane 15), M1 (lane 8), and M17 (lane 23), but no effect with wt 3AB (lane 5). In the presence of 200-fold excess of nonlabeled competitor, only wt, M6, and M19 3ABs were able to form an RNP complex, albeit at greatly reduced yield (lanes 6, 12, and 30, respectively). The nature of the slower migrating bands in lanes 7, 8, 13, and 14 is not known. They could represent smaller RNP complexes formed only with the certain mutant 3ABs (see below). Roughly estimated, the ability of forming [3AB/3CD^{PRO}/cloverleaf]-RNPs can be listed as: M18 < M14 < (M17 < M1, M10, M11) < (M6, M19, wt).

Significantly, the results from the two assays are generally consistent with each other: the most drastic effects were observed with changes of positive charge in 3AB mutants mapping to the 3B portion of the polypeptide. This strongly suggests that the 3B (VPg) domain of 3AB plays an important role in nonspecific RNA binding as well as in the formation of the 5'-terminal RNP complex.

As discussed previously (Harris et al., 1994; Xiang et al., 1995), we cannot explain at present the nature

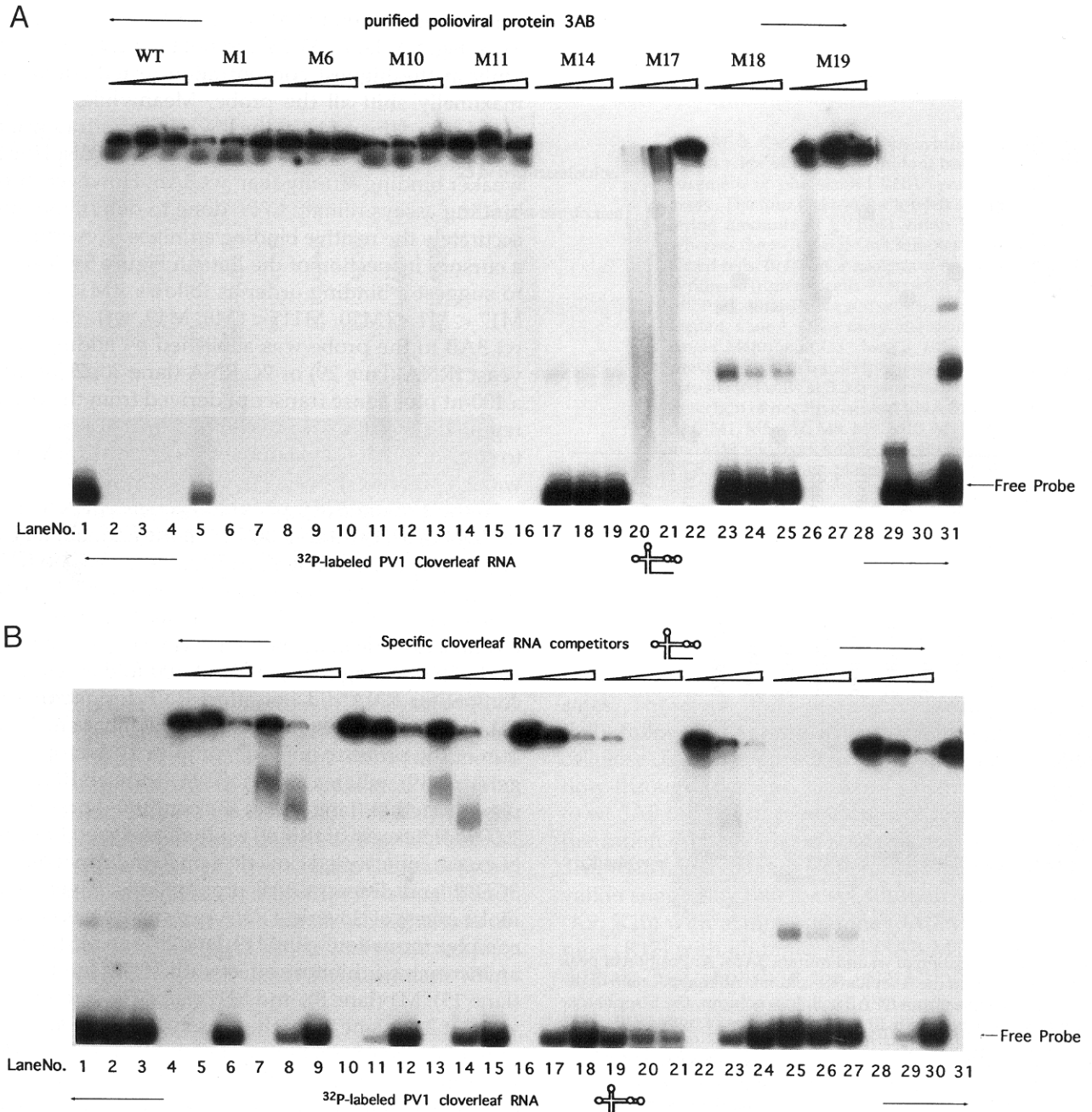


FIGURE 5. Nonspecific RNA-binding and specific RNP-forming activities of wt and mutant 3AB proteins; 20,000 cpm of of ³²P-labeled PV1(M) cloverleaf probe (100 nt) was present in each reaction. **A:** Nonspecific RNA-binding activities of wt and mutant 3AB proteins. Lanes 2–28 represent gel-shift assays, each with wt or mutant 3AB (0.4, 0.8, and 1.6 μ M); lanes 1 and 31, cloverleaf probe in binding buffer without protein factors; lanes 29 and 30, 1.6 μ M wt 3AB (as in lane 4) incubated with 15 μ g of yeast tRNA or 1.63 μ g (20 molar excess over the RNA probe) of 2C RNA (a 100-nt transcript derived from poliovirus protein 2C coding region), respectively. **B:** Specific RNP-forming activities of wt and mutant 3AB proteins. Each reaction contains 15 μ g (about 1,000 molar excess over the RNA probe) of yeast tRNA. Lanes 4–30 represent gel-shift assays, each with 0.2 μ M of purified PV2 (Sabin) 3CD^{Pro}, 0.8 μ M of wt (lanes 4–6), or mutant 3AB (M1, lanes 7–9; M6, lanes 10–12; M10, lanes 13–15; M11, lanes 16–18; M14, lanes 19–21; M17, lanes 22–24; M18, lanes 25–27; M19, lanes 28–30), and increasing amount of full-length cloverleaf RNA competitor (0, 20, or 200 molar excess over the RNA probe); lane 1, cloverleaf probe in binding buffer and tRNA without protein factors; lanes 2 and 3, same as in lane 1 except 0.8 μ M of wt 3AB or 0.2 μ M of 3CD^{Pro} was added; lane 31, same as in lane 4 except 200 molar excess of 2C RNA was added.

of the large 3AB/3CD^{Pro}/cloverleaf complexes that are retained at the top of the nondenaturing polyacrylamide gels. 3AB is a highly charged polypeptide and yet, it is water insoluble, presumably due to a strong

hydrophobic domain (Fig. 2A). Even in the presence of detergent (Nonidet P-40), 3AB has the tendency to form dimers and oligomers (Lama et al., 1994). We speculate the 3AB/3CD^{Pro}/cloverleaf complex is sur-

rounded by detergent molecules that, altogether, form large entities that are unable to enter the gel matrix.

Stimulation of 3CD^{pro} cleavage during in vitro translation

In studies of in vitro processing of the poliovirus polypeptide, it has been shown that addition of antibodies to VPg inhibits, whereas addition of purified 3AB protein stimulates, proteolysis of 3CD^{pro} to 3C^{pro} and 3D^{pol} (Molla et al., 1994). This effect has been reproduced using the purified polypeptides 3CD^{pro} and 3AB, an observation suggesting that binding of 3AB to 3CD^{pro} stimulates autoproteolysis (Molla et al., 1994).

In an attempt to map the region(s) of 3AB involved in the accelerated cleavage of 3CD^{pro}, assays similar to those described by Molla et al. (1994) were carried out with purified 3AB mutants (see the Materials and methods). Molla et al. (1994) have shown that addition of 3AB to a HeLa cell extract does not stimulate the overall translational efficiency. We have confirmed this in our translation experiments (data not shown). The signals corresponding to 3C^{pro} (the cleavage product of 3CD^{pro}) on the exposed film were subjected to laser scanning and the intensity of each band was quantified. As seen in Figure 6, accumulation of 3C^{pro} in-

creased with the increasing amount of exogenous wt 3AB added. Stimulation was similar albeit somewhat lower with mutant 3ABs M1, M10, M11, and M19. In contrast, M6, and particularly M14, M17, and M18, not only failed to stimulate 3CD^{pro} processing, but appeared to inhibit it. Thus, the 3AB mutants affected the 3CD^{pro} processing, to different extents in the rough order: (M14, M18) < M6 < M17 < (M10, M11) < (M1, M19, wt).

Stimulation of 3D^{pol} polymerase activity in vitro by 3AB

We have shown previously that under a certain set of reaction conditions the synthesis of poly(U) by 3D^{pol} on a poly(A) template with oligo(dT)₁₅ as primer is stimulated by the addition of 3AB as much as 50 to 100-fold (Paul et al., 1994a). The exact mechanism of stimulation is not known, but it probably depends on the ability of 3AB to interact both with the template poly(A) (Paul et al., 1994a) and with 3D^{pol} (Molla et al., 1994).

It was of interest to find out whether this phenomenon, observed in vitro, had any biological significance for poliovirus replication. One possible way was to analyze the mutant 3ABs for their ability to stimulate poly(U) synthesis by 3D^{pol} using this in vitro assay.

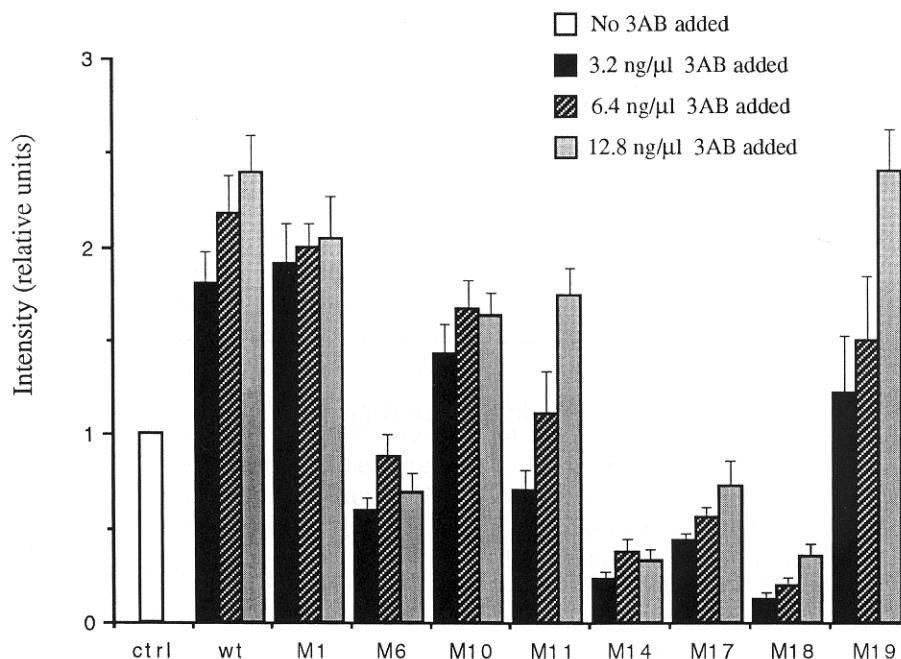


FIGURE 6. Stimulation of 3CD^{pro} autocleavage by purified wt or mutant 3ABs during in vitro translation of poliovirus RNA. Poliovirus RNA was translated in HeLa cell free extracts (see the Materials and methods) for 15 h at 30 °C either in the absence or presence of purified 3AB (3.2–12.8 μg/mL), the total volume of each reaction is 12.5 μL. An aliquot (6 μL) was analyzed on a 13.5% SDS-polyacrylamide gel (see the Materials and methods). The intensity of the 3C^{pro} band on the X-ray film was quantified by the Scan Analysis program (Biosoft). The open, black, striped, and gray columns show the units of 3C^{pro} released from 3CD^{pro} in the presence of 0, 3.2, 6.4, and 12.8 μg/mL of purified wt or mutant 3AB, respectively. One unit is defined as the intensity of the 3C^{pro} band generated from autocleavage of 3CD^{pro} in the absence of exogenously added 3AB. Means shown are means of three independent experiments.

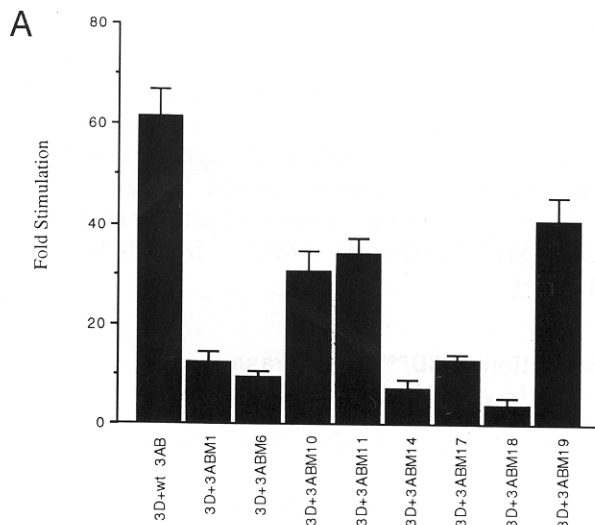
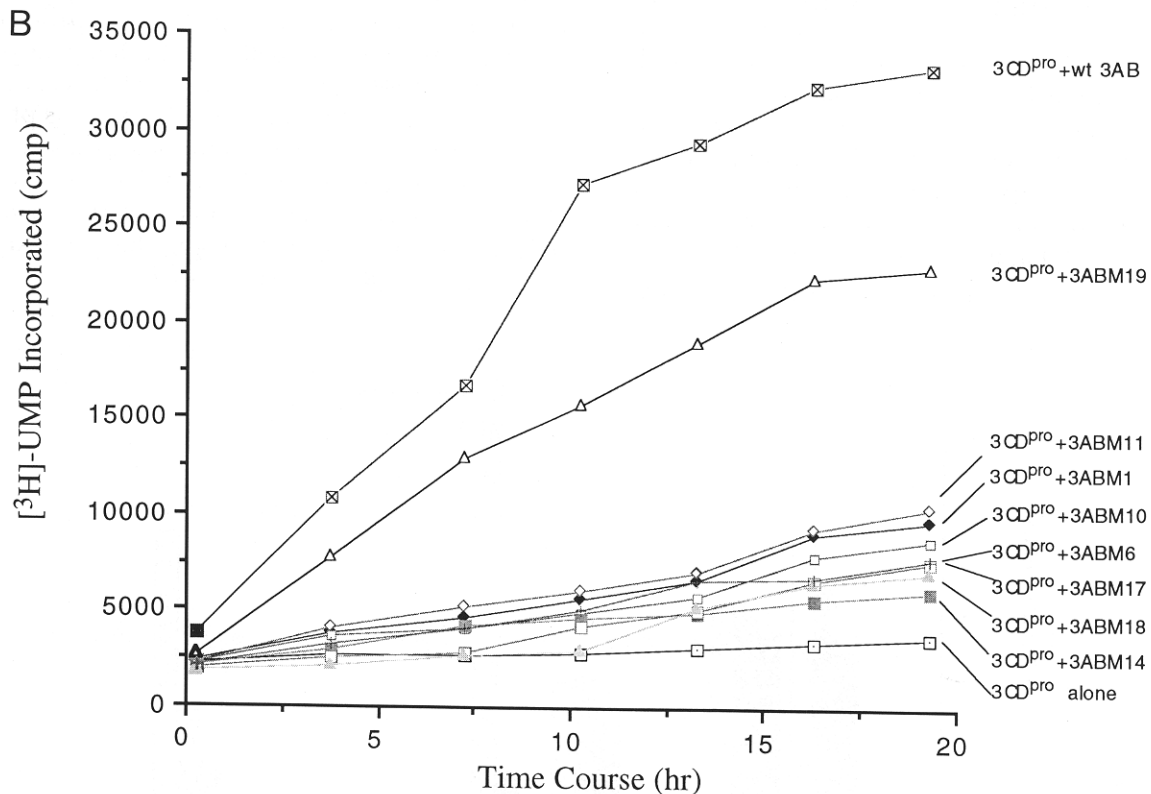


FIGURE 7. A: Stimulation of 3D^{pol} catalyzed poly(U) synthesis in vitro by wt and mutant 3AB polypeptides. Poly(U) synthesis by 3D^{pol} (2.7 nM) was measured either in the absence or presence of purified wt or mutant 3ABs (1 μ M), as described in the Materials and methods. Fold stimulation was calculated from the ratio of counts obtained in the presence and absence of 3AB. Values are means of triplicate of three independent assays. **B:** Effect of wt and mutant 3ABs on 3CD^{pro} autocleavage-dependent 3D^{pol} activity. 3CD^{pro} autocleavage was conducted as described in the Materials and methods with 40 μ g/ μ l 3CD^{pro} and 50 μ g/ μ l purified wt or mutant 3ABs added. The mixture was incubated at 30 °C for a total of 18 h and 5- μ l aliquots were removed at the time points indicated on the figure. All samples were stored at -20 °C until analyzed by the standard polymerase assay in triplicate (see the Materials and methods). Values plotted here represent an average of three samples.



Our results indicate that none of the mutant 3ABs were able to stimulate 3D^{pol} to the same extent as the wt protein (Fig. 7A). The most striking reduction in enhancement can be seen with M18 and M14, mutants in VPg, whose stimulatory effect was reduced 15- and 8-fold, respectively. Similarly affected was M6, with a mutation in the 3A portion of 3AB that exhibited a 7-fold reduction in stimulatory activity. The stimulatory activity of all the mutants tested can be summarized as follows: M18 < M14 < M6 < M1 < M17 < M10 < M11 < M19 < wt.

Synergistic effect of 3AB mutants on 3CD^{pro} autocleavage and 3D^{pol} activity

Incubation of purified 3AB and 3CD^{pro} results in enhanced autocleavage of 3CD^{pro} yielding 3C^{pro} and 3D^{pol}. Subsequently, the polymerase activity of 3D^{pol} could be stimulated by complexing to 3AB, and such activity can be readily detected in vitro (Molla et al., 1994). The synergistic effect of such consequential events shall reflect the RNA replication activity of a specific 3AB mutant construct in vivo.

We have used the same analysis to measure the synergistic effect of 3AB mutants on 3D^{pol} activity resulting from self-cleavage of 3CD^{pro}. Figure 7B shows a progressive increase of polymerase activity during the incubation of 3CD^{pro} with wt 3AB, which is hardly detectable when 3CD^{pro} is incubated alone. Using this two-step assay, only 3AB M19 was found to have a comparable effect on 3D^{pol} activity as the wt protein. Interestingly, M1 and M19 showed similar activities in 3CD^{pro} cleavage (Fig. 6), whereas M1 exhibited much less synergistic activity than M19, which is due to much repressed stimulation on 3D^{pol}. The synergistic effect of the mutant proteins can be summarized as: (M14 < M18 < M17 < M6 < M10 < M1 < M11) < M19 < wt.

DISCUSSION

We have recently described several different functions of the poliovirus protein 3AB that implicate this polypeptide, apart from being a precursor for VPg, as playing an important role in various steps of poliovirus genome replication (Harris et al., 1994; Lama et al., 1994; Molla et al., 1994; Paul et al., 1994a; Xiang et al., 1995). These functions appear to involve protein-protein interactions as well as RNA binding. A clustered charged-to-alanine mutagenesis algorithm seemed well suited to identify those domains of the polypeptide involved in the different functions (Wertman et al., 1992). It seemed likely that this strategy would yield conditional lethal poliovirus mutants (with a *ts* phenotype) and, indeed, *ts* mutants mapping to 3D^{pol} have been generated in this way (Diamond & Kirkegaard, 1994). No *ts* mutants, however, were found among the 3AB mutants described here. The mutants generated had phenotypes falling into three categories: (1) small plaque, impaired in RNA synthesis (M7, 8, 9); (2) lethal, low level of RNA synthesis (M19); and (3) lethal, no RNA synthesis (M1, 6, 10, 11, 14, 17, 18). For the viable virus in category 1, we have passaged the viruses four times. No revertant was generated inside the 3AB coding region. As pointed out before, we have not yet determined whether the mutations in the 3AB coding regions or some second-site mutations are responsible for the observed phenotypes. It should be noted that a previous report regarding mutants M17 and M18 is at variance with our data described here in that RNA synthesis was found in cells transfected with M17 or M18 transcripts (Reuer et al., 1990). We cannot explain this discrepancy at present, but we believe that it is possibly due to a different method of sample preparations yielding high backgrounds in the older study.

It is apparent that the lethal mutations described here map to both the 3A and VPg (=3B) domains of 3AB. In the absence of detectable RNA replication, a search for second-site revertants seemed likely to fail and, so far, has not been pursued. We cannot rule out the possibility that one or the other lethal mutant is, in fact, quasi-infectious (Cao & Wimmer, 1995a), and ca-

pable of (second-site) reversion at a very low rate. An explanation of the lethal phenotype and its relation to the domain structure of 3AB made it necessary, therefore, to purify the mutant proteins and employ them in functional assays of RNA binding and interactions with polypeptides 3CD^{pro} and 3D^{pol}.

The purification of the mutant 3ABs revealed the interesting phenomenon that the elimination of basic residues in the 3B domain of polypeptides M14 and M18 completely abrogated the mutant protein's ability to bind to S-sepharose, a cation exchange resin. None of the other mutant proteins with a similar overall-reduced net positive charge showed the same properties. It is possible that the mutations M14 and M18 altered the conformation of the proteins, thereby masking several positive charges. Alternatively, the 3B domain may be highly exposed in contrast to basic residues in other regions, and thus serve as dominant domain for interactions with cation exchange resins or with viral macromolecules. The latter is likely true for 3AB's ability to function as a nonspecific RNA-binding protein because 3AB M14 and M18 have lost this property.

The purified mutant proteins were used in a series of functional assays *in vitro*: RNA binding, formation of a [3AB/3CD^{pro}/cloverleaf]-RNP, stimulation of 3CD^{pro} processing, and stimulation on 3D^{pol} polymerase activity. The results of these assays are summarized in Figure 2B. Significantly, the M14 and M18 mutant proteins, both of which failed to bind to S-sepharose column, exhibited the highest degree of functional loss in all these assays. In M18, the single Arg was changed to Glu (R17E) with most dramatic consequences; changes at this position to Gln (M17) or Lys (M19) exhibited less of an effect, an observation implying that electrostatic changes, rather than conformational alterations, were possibly the cause of changes in activity.

Mutant M19 protein retained most of the activities assayed *in vitro*, and full-length RNA transcripts carrying this lesion showed RNA synthesis on transfection in HeLa cells. However, the mutation was lethal, a phenotype that we cannot explain at present. Whether this mutation can be rescued by genetic complementation is currently under investigation.

A number of different motifs have been identified in proteins capable of binding to RNA (Kenan et al., 1991; Dreyfuss et al., 1993; Mattaj, 1993), but poliovirus 3AB does not contain any of these typical RNA-binding motifs. The positively charged sites in the VPg domain, however, appear to play a role in RNA binding because their alteration to neutral or acidic residues reduces or abolishes this property. Indeed, in VPg sequences of all entero- and rhinoviruses, two closely related genera of Picornaviridae, these basic residues are conserved. Generally, reduction in nonspecific RNA-binding activity co-varies with a reduction in the ability of the corresponding 3AB to stimulate 3D^{pol} polymerase activity. Exceptions are mutant proteins M6 and, to a lesser extent, M11. These exceptions are of particular interest

for our studies of the molecular basis of stimulation of 3D^{pol} activity by wt 3AB (Paul et al., 1994a). 3AB M17 is also an exception in that it is weak in nonspecific RNA binding, but strongly promotes the formation of [3AB/3CD^{pro}/cloverleaf]-RNP. Apparently, this RNP formation involves protein-protein interactions that differ from that of the RNA-protein interaction.

The role of the Arg residue (R17 of VPg) close to the C-terminus of 3AB deserves special mention with regard to a transcriptional event in *Bacillus subtilis* phage ϕ 29. The small P4 protein of ϕ 29 has been shown to contact the phage RNA polymerase and stabilizes the binding of the latter to DNA, thereby activating transcription from the viral late promoter, P_{A3}. Like 3AB, P4 has an arginine residue near its highly basic C-terminus. A substitution of this residue to glutamine gives rise to a P4 protein unable to activate transcription. The mutant protein does not form a complex with the RNA polymerase, therefore abrogating stimulation of the binding of RNA polymerase to the promoter (Mencia et al., 1993).

In contrast to the drastic consequences of the mutations in the VPg domain of 3AB, the clustered charged-to-alanine mutants (M1, M6, M10, M11) in the 3A domain, although lethal, generally showed less deleterious effects. All retained near normal RNA-binding and specific RNP complex-forming activities. Of the four 3AB proteins, only M6 was totally defective in stimulating 3CD^{pro} cleavage, whereas M1 and M6 displayed much reduced ability to stimulate 3D^{pol} activity. The most striking result with all four mutant proteins could be observed with the assay measuring the synergistic effect of 3CD^{pro} cleavage and 3D^{pol} stimulation. Although a synthetic 3A peptide failed to show distinctive activities in vitro (Molla et al., 1994; Paul et al., 1994a), hundreds-fold molar excess of VPg was required to obtain the similar activities of wt 3AB (Molla et al., 1994; Paul et al., 1994a; unpubl. data in our group). All these observations demonstrate that the function of VPg could be maximized only in the context of 3AB. The N-terminal part of 3A, with its functional conformation as well as its charged regions, contributes indispensably to the overall function of 3AB. In the case of 3CD^{pro} or 3D^{pol} interaction, the N-terminal part of 3AB may be in the vicinity of the VPg portion, allowing some site(s) (especially M6 site) in 3A to participate in protein-protein association. Analyses in the yeast two-hybrid system may reveal subtle differences in the binding of these proteins with 3CD^{pro}, 3D^{pol}, or other virus-specific polypeptides. Experiments to this effect are in progress.

MATERIALS AND METHODS

Construction of mutant plasmids

To create subclones of 3AB-encoding poliovirus sequences suitable for site-directed mutagenesis, the DNA segment

spanning the unique *Mlu* I (nt 4830) and *Bgl* II sites (nt 5600) in plasmid pT7PVM1 (Cao & Wimmer, 1995) was amplified by PCR. PCR products introduced additional *Sac* I and *Sal* I sites outside poliovirus-specific sequences. Products were digested with *Sac* I and *Sal* I (New England Biolab) and were subcloned into pBluescript KS(+) phagemid (Stratagene), utilizing the *Sac* I and *Sal* I sites.

Deoxyoligonucleotide mutagenesis was performed according to the method of Kunkel et al. (1987). In the sequences of deoxyoligonucleotides given below, sequences for introduced alanine codons are underlined and the nucleotides that differ from the sequence of poliovirus are shown in bold face. The mutagenic deoxyoligonucleotides used were: GAGATTA CTGTGCGGCGGCGGGTTGGATAG (3AB-M1); CCACTC CAGTATGCGGCGTTGAAAATTGAC (3AB-M6); CCCAGG AGGTGGCGGCGTACTGTGAGAAG (3AB-M7); GCCAG GTTCAAACAGCGGCGAACATCAACAGGC (3AB-M8); CCAGTATAAAGACTTGGCGATTGCGATCGCGACGAGT CCC (3AB-M9); CCCCCTCTCGGTGTATCAATGCGTTGC TCCAA (3AB-M10); CCAAGCAGTTGCGTCCCAGGCCGT GAGCATTACTG (3AB-M11); GGTTTACCAAACGCGGCG CCAAC GTGCCC (3AB-M14).

The poliovirus mutant plasmids pT7VPg17, pT7VPg18, and pT7VPg19 were constructed by Kuhn et al. (1988b) and are renamed here pT7PV1-3AB-M17, pT7PV1-3AB-M18, pT7PV1-3AB-M19, respectively. All three constructs also contained an additional VPg K10R substitution for the construction of the mutagenesis cartridge. The Lys to Arg substitution alone showed wt phenotype (Kuhn et al., 1988a).

The 3AB-encoding sequences of each mutagenized plasmid were excised by digestion with *Mlu* I and *Bgl* II and cloned back into the infectious cDNA clone pT7PVM. To express the recombinant mutant 3ABs, the encoding DNA fragments were amplified by oligo 1 (GCTTTGCATATGGACCACTC CAGTATACTTGCTGTCCGAAT) and oligo 2 (CCGGGGTG ATCACTTTGCTGTCCGAAT), except that the ones encoding 3AB-M17~19 were amplified by oligo 1 and oligo 3 (CCG GGGTGATCACTTTGCTGT). All the fragments were digested with *Bcl* I and *Nde* I and inserted into the protein expression vector pET11b, which had been digested with *Bam*H I and *Nde* I. The resulting clones were transformed into *E. coli* BL21(DE3) strain. The presence of the introduced mutations in either subclones or full-length cDNA clones was verified by DNA sequencing.

In vitro transcription and in vitro translation

Prior to transcription with T7 RNA polymerase, the wt or mutant full-length cDNA clones were linearized with *Eco*R I. Conditions for the in vitro transcription have been described previously (van der Werf et al., 1986). Equal amounts of RNA transcripts were used to program HeLa cell translation extracts (Molla et al., 1991). After incubation overnight at 30 °C, aliquots of samples labeled with [³⁵S] translabel were analyzed by electrophoresis on 12.5% SDS-polyacrylamide gels, followed by autoradiography.

RNA transfection and plaque assay

All assays were performed with R19 HeLa cell monolayers maintained in Dulbecco modified eagle medium supplemented with 2% bovine calf serum (GIBCO). The transcript

RNAs from *in vitro* transcription were used for RNA transfections, which were carried out by the DEAE-Dextran method (Kuhn et al., 1988b). Cell lysates harvested from transfected cell were subjected to plaque assay.

Detection of viral RNA synthesis

To detect plus-strand RNA synthesis, HeLa cell monolayers (2×10^6 cells) were transfected with one of the RNA transcripts. All steps, from RNA extraction to hybridization, were carried out according to procedures described previously (Paul et al., 1994b). Briefly, one half of the extracted intracellular RNAs was used in the assay. A 98-nt riboprobe, complementary to 5' end of plus-strand RNA, was labeled with [α - 32 P]UTP and used for hybridization at 50 °C.

To detect minus-strand RNA synthesis, one tenth of the RNA samples extracted from the cells 25 h after transfection was treated with RNase-free DNase I for 1 h to eliminate the DNA contamination and then preheated at 100 °C for 5 min to separate the minus-strand RNA from the plus strand. Using oligo 4 (5' AGTCTGGTGCCCGCTCCACC 3', nt 3280–3300 of PVM cDNA), the reverse transcription reactions were conducted by Tth polymerase at 75 °C for 20 min, followed by digestion with RNase A (10 μ g) for 15 min at 37 °C. The cDNAs were amplified by PCR using Taq polymerase with oligo 4 and oligo 5 (5' CCTGAGTGCCCAAGTGGTAGTTGC 3'), complementary to nt 3435–3458 of PVM cDNA). Twenty-five amplification cycles were performed, each cycle consisting of 45 s of denaturation at 94 °C, 45 s of annealing at 60 °C, and 1 min of polymerization at 72 °C. All enzymes used in this assay were from Boehringer Mannheim.

Protein purification

Purification of poliovirus 3AB has been described (Lama et al., 1994). Briefly, the membrane-bound wt or mutant 3ABs were solubilized with detergent Nonidet P-40 and subjected to two chromatographic steps. First, the fraction of flow through was collected from the DEAE-cellulose column (Whatman) at pH 8.5. Second, it was applied onto S-Sepharose fast flow column (Pharmacia), which was then washed subsequently with 10 column volumes of buffer S10, S100, and S200 (which contained 10, 100, and 200 mM NaCl, respectively). For the mutant 3ABs, each eluent was fractionated in 1-ml aliquots, and the peak of eluent was detected by the SDS-PAGE.

RNA-binding assay

RNA gel-shift analyses were carried out as described previously (Harris et al., 1994), each 25- μ L reaction containing 20,000 cpm of [α - 32 P]UTP-labeled PV1(M) cloverleaf RNA. The binding buffer consisted of 5 mM MOPS, pH 7.4, 25 mM KCl, 2 mM MgCl₂, 20 mM DTT. The final concentration of purified 3CD^{pro} (encoded from PV2 [Sabin] with a T181K cleavage site mutation repressing its autocleavage activity, whereas its proteinase and RNA-binding activities are not affected, see Harris et al., 1992) was kept constant at 0.2 μ M, whereas that of purified 3AB was 0.4, 0.8, or 1.6 μ M. In some reactions, nonspecific RNA competitor includes 15 μ g of tRNA from Baker's yeast (Boehringer Mannheim) or 1.63 μ g

of 2C RNA (a transcript derived from polioviral 2C coding region) was added. In specific competition assays, full-length cloverleaf RNA was added that was 20 or 200 molar excess over the RNA probe.

In vitro translation and cleavage assay

As described previously (Molla et al., 1991), 200 ng of purified poliovirus RNA was translated in a HeLa cell extract in the presence of [35 S]-translabel. For cleavage assays, various amount of purified wt or mutant 3AB was added to the 12.5- μ L translation reactions and incubated at 30 °C for 15 h. The samples were then analyzed by SDS-PAGE and subjected to autoradiography. An aliquot (6 μ L) was analyzed on a 13.5% SDS-polyacrylamide gel (see the Materials and methods). The intensity of the 3C^{pro} band on the X-ray film was quantified by the Scan Analysis program (Biosoft).

Polymerase assay

3D^{pol} was assayed by measuring poly(U) synthesis on a poly(A) template similar to the method of Van Dyke and Flanagan (1980). As described previously (Lama et al., 1994; Paul et al., 1994a), the reaction mixture (25 μ L), optimized for measuring the stimulatory activity of 3AB on 3D^{pol}, contained: 50 mM HEPES, pH 7.8, 3 mM MgCl₂, 10 mM dithiothreitol, 125 ng oligo(dT)₁₅, 0.5 μ g of poly(A), 1 μ Ci of [3 H]-UTP (43 Ci/mmol, ICN), 0.1% Nonidet P40, and 3.5 ng (2.7 nM) of purified 3D^{pol} (a generous gift from Dr. Stephen J. Plotch). When indicated, 12 μ g/mL (1 μ M) of 3AB was added. The mixture was incubated for 1 h at 37 °C.

3CD^{pro} autocleavage and 3D^{pol} polymerase assay

In a 3CD^{pro} reaction buffer (20 mM HEPES, pH 7.4, 100 mM NaCl, 1 mM Na₃EDTA, and 1 mM DTT), 40 μ g/mL of purified 3CD^{pro} was incubated with 50 μ g/mL purified wt or mutant 3ABs at 30 °C for 18 h. At each time point, 5 μ L of the sample was removed and stored at -20 °C. Each sample was analyzed by standard polymerase assay.

ACKNOWLEDGMENTS

Purified 3D^{pol} was a generous gift from Dr. Stephen J. Plotch. W.X. is a member of the graduate training program in biochemistry and cell biology. A.C. is a member of graduate training program in molecular genetics and microbiology. This work was supported by grants PN9329(HFSPO), AI15122, and AI32100.

Received July 31, 1995; returned for revision September 9, 1995; revised manuscript received October 17, 1995

REFERENCES

- Alexander L, Lu HH, Wimmer E. 1994. Polioviruses containing picornavirus type and/or type 2 internal ribosomal entry site elements: Genetic hybrids and the expression of a foreign gene. *Proc Natl Acad Sci USA* 91:1406–1410.

- Andino R, Rieckhof GE, Baltimore D. 1990a. A functional ribonucleo-protein complex forms around the 5' end of poliovirus RNA. *Cell* 63:369-380.
- Andino R, Rieckhof GE, Trono D, Baltimore D. 1990b. Substitutions in the protease (3C^{pro}) gene of poliovirus can suppress a mutation in the 5' noncoding region. *J Virol* 64:607-612.
- Bernstein HD, Baltimore D. 1988. Poliovirus mutant that contains a cold-sensitive defect in viral RNA synthesis. *J Virol* 62:2922-2928.
- Bernstein HD, Sarnow P, Baltimore D. 1986. Genetic complementation among poliovirus mutants derived from an infectious cDNA clone. *J Virol* 60:1040-1049.
- Bienz K, Egger D, Troxler M, Pasamontes I. 1990. Structural organization of poliovirus RNA replication is mediated by viral proteins of the P2 genomic region. *J Virol* 64:1156-1163.
- Borman AM, Deliat FG, Kean KM. 1994. Sequences within the poliovirus internal ribosome entry segment control viral RNA synthesis. *EMBO J* 13:3149-3157.
- Cao X, Wimmer E. 1995a. Intragenomic complementation of a 3AB mutant in dicistronic polioviruses. *Virology* 209:315-326.
- Cao X, Wimmer E. 1995b. Genetic variation of the poliovirus genome with two VPg coding units. *EMBO J*. Forthcoming.
- Cao XM, Kuhn RJ, Wimmer E. 1993. Replication of poliovirus RNA containing two VPg genes leads to a specific deletion event. *J Virol* 67:5572-5578.
- Datta U, Dasgupta A. 1994. Expression and subcellular localization of poliovirus VPg-precursor protein 3AB in eukaryotic cell: Evidence for glycosylation in vitro. *J Virol* 68:4468-4477.
- Diamond S, Kirkegaard K. 1994. Clustered charged-to-alanine mutagenesis of poliovirus RNA-dependent RNA polymerase yields multiple temperature-sensitive mutants defective in RNA synthesis. *J Virol* 68:863-876.
- Dreyfuss G, Matunis MJ, Pinol-Roma S, Burd CG. 1993. HnRNP proteins and biogenesis of mRNA. *Annu Rev Biochem* 62:289-321.
- Giachetti C, Hwang SS, Semler BL. 1992. Cis-acting lesions targeted to the hydrophobic domain of a poliovirus membrane protein involved in RNA replication. *J Virol* 66:6045-6057.
- Giachetti C, Semler BL. 1991. Role of a viral membrane polypeptide in strand-specific initiation of poliovirus RNA synthesis. *J Virol* 65:2647-2654.
- Harris KS, Hellen CUT, Wimmer E. 1990. Proteolytic processing in the replication of picornaviruses. *Sem Virol* 1:323-333.
- Harris KS, Reddigari SR, Nicklin MJH, Hämmerle T, Wimmer E. 1992. Purification and characterization of poliovirus polypeptide 3CD, a proteinase and a precursor for RNA polymerase. *J Virol* 66:7481-7489.
- Harris KS, Xiang W, Alexander L, Paul AV, Lane WS, Wimmer E. 1994. Interaction of the polioviral polypeptide 3CD^{pro} with the 5' and 3' termini of the poliovirus genome: Identification of viral and cellular cofactors necessary for efficient binding. *J Biol Chem* 269:27004-27014.
- Jacobson SJ, Konings DAM, Sarnow P. 1993. Biochemical and genetic evidence for a pseudoknot structure at the 3' terminus of the poliovirus RNA genome and its role in viral RNA amplification. *J Virol* 67:2961-2971.
- Jang SK, Kräusslich HG, Nicklin MJH, Duke GM, Palmenberg AC, Wimmer E. 1988. A segment of the 5' nontranslated region of encephalomyocarditis virus RNA directs internal entry of ribosomes during in vitro translation. *J Virol* 62:2636-2643.
- Kenan DJ, Query CC, Keene JD. 1991. RNA recognition: Towards identifying determinants of specificity. *Trends Biochem Sci* 16:214-220.
- Kuge S, Nomoto A. 1987. Construction of viable deletion and insertion mutants of the Sabin strain type 1 poliovirus: Function of the 5' noncoding sequence in viral replication. *J Virol* 61:1478-1487.
- Kuhn RJ, Tada H, Ypma WM, Dunn JJ, Semler BL, Wimmer E. 1988a. Construction of a "mutagenesis cartridge" for poliovirus genome-linked viral protein: Isolation and characterization of viable and nonviable mutants. *Proc Natl Acad Sci USA* 85:519-523.
- Kuhn RJ, Tada H, Ypma-Wong MF, Semler BL, Wimmer E. 1988b. Mutational analysis of the genome-linked protein VPg of poliovirus. *J Virol* 62:4207-4215.
- Kunkel T, Roberts JD, Zakour RA. 1987. Rapid and efficient site-specific mutagenesis without phenotypic selection. *Methods Enzymol* 154:367-382.
- Lama J, Paul AV, Harris KS, Wimmer E. 1994. Properties of purified recombinant poliovirus protein 3AB as substrate for viral proteinases and as co-factor for viral polymerase 3D^{pol}. *J Biol Chem* 269:66-70.
- Lawson MA, Semler BL. 1992. Alternate poliovirus nonstructural protein processing cascades generated by primary sites of 3C proteinase cleavage. *Virology* 191:309-320.
- Mattaj JW. 1993. RNA recognition: A family matter? *Cell* 73:837-840.
- Mencia M, Salas M, Rojo F. 1993. Residues of the *Bacillus subtilis* phage ϕ 29 transcriptional activator required both to interact with RNA polymerase and to activate transcription. *J Mol Biol* 233:695-704.
- Molla A, Harris KS, Paul AV, Shin SH, Mugavero J, Wimmer E. 1994. Stimulation of 3C^{pro}-related proteolysis by the genome-linked protein, VPg, and its precursor, 3AB. *J Biol Chem* 269:27015-27020.
- Molla A, Paul AV, Wimmer E. 1991. Cell-free, de novo synthesis of poliovirus. *Science* 254:1647-1651.
- Nomoto A, Morgan-Detjen B, Pozzatti R, Wimmer E. 1977. The location of the polio genome protein in viral RNAs and its implication for RNA synthesis. *Nature* 268:208-213.
- Novak JE, Kirkegaard K. 1991. Improved method for detecting negative strands used to demonstrate specificity of plus strand encapsidation and the ratio of positive to negative strands in infected cells. *J Virol* 65:3384-3387.
- Paul A, Cao X, Harris KS, Lama J, Wimmer E. 1994a. Studies with poliovirus polymerase 3D^{pol}: Stimulation of poly(U) synthesis in vitro by purified poliovirus protein 3AB. *J Biol Chem* 269:29173-29181.
- Paul AV, Molla A, Wimmer E. 1994b. Studies of a putative amphipathic helix in the N-terminus of poliovirus protein 2C. *Virology* 199:188-199.
- Pelletier J, Sonenberg N. 1988. Internal initiation of translation of eukaryotic mRNA directed by a sequence derived from poliovirus RNA. *Nature* 334:320-325.
- Pilipenko EV, Maslova SV, Sinyakov AN, Agol VI. 1992. Towards identification of cis-acting elements involved in the replication of enterovirus and rhinovirus RNAs: A proposal for the existence of tRNA-like terminal structures. *Nucleic Acids Res* 20:1739-1745.
- Racaniello VR, Meriam C. 1986. Poliovirus temperature-sensitive mutant containing a single nucleotide deletion in the 5'-noncoding region of the viral RNA. *Virology* 155:498-507.
- Reuer Q, Kuhn RJ, Wimmer E. 1990. Characterization of poliovirus clones containing lethal and nonlethal mutations in the genome-linked protein VPg. *J Virol* 64:2967-2975.
- Rivera VM, Welsh JD, Maizel JV. 1988. Comparative sequence analysis of the 5' noncoding region of the enteroviruses and rhinoviruses. *Virology* 165:42-50.
- Rohll JB, Percy N, Ley R, Evans DJ, Almond JF, Barclay WS. 1994. The 5'-untranslated regions of picornavirus RNAs containing independent functional domains essential for RNA replication and translation. *J Virol* 68:4384-4391.
- Semler B, Anderson C, Hanecak R, Dorner L, Wimmer E. 1982. A membrane-associated precursor to poliovirus VPg identified by immunoprecipitation with antibodies directed against a synthetic heptapeptide. *Cell* 28:405-412.
- Takeda NR, Kuhn J, Yang CF, Takegami T, Wimmer E. 1986. Initiation of poliovirus plus strand RNA synthesis in a membrane complex of infected HeLa cells. *J Virol* 60:43-53.
- Takegami T, Kuhn RJ, Anderson CW, Wimmer E. 1983. Membrane-dependent uridylylation of the genome-linked protein VPg of poliovirus. *Proc Natl Acad Sci USA* 80:7447-7451.
- van der Werf S, Bradley J, Wimmer E, Studier FW, Dunn JJ. 1986. Synthesis of infectious poliovirus RNA by purified T7 RNA polymerase. *Proc Natl Acad Sci USA* 83:2330-2334.
- Van Dyke TA, Flanagan J. 1980. Identification of poliovirus polypeptide p63 as a soluble RNA-dependent RNA polymerase. *J Virol* 35:732-740.
- Wertman KF, Drubin DG, Botstein D. 1992. Systematic mutational analysis of the yeast ACT1 gene. *Genetics* 132:337-350.
- Wimmer E, Hellen CUT, Cao XM. 1993. Genetics of poliovirus. *Annu Rev Genet* 27:353-436.
- Xiang W, Harris KS, Alexander L, Wimmer E. 1995. Interaction between the 5'-terminal cloverleaf and 3AB/3CD^{pro} of poliovirus is essential for RNA replication. *J Virol* 69:3658-3667.